NUP145 Encodes a Novel Yeast Glycine–Leucine–Phenylalanine–Glycine (GLFG) Nucleoporin Required for Nuclear Envelope Structure

Susan R. Wente and Günter Blobel

Laboratory of Cell Biology, Howard Hughes Medical Institute, The Rockefeller University, New York 10021

Abstract. We have isolated and characterized the gene encoding a fourth yeast glycine–leucine–phenylalanine–glycine (GLFG) repeat nucleoporin with a calculated molecular mass of 145.3 kD, and therefore termed *NUP145*. The amino-terminal half of Nup145p is similar to two previously identified GLFG nucleoporins, Nup116p and Nup100p (Wente, S. R., M. P. Rout, and G. Blobel. 1992. *J. Cell Biol.* 119:705–723). A deletion/disruption in the amino-terminal half of *NUP145* (*nup145ΔN*) had only a slight effect on cell growth at temperatures between 17 and 37°C. However, immunofluorescence microscopy of *nup145ΔN* cells with antinucleoporin antibodies showed that the characteristic punctate nuclear staining normally seen in wild-type yeast cells was reduced, with the majority of the signal located in one or two intense spots at the nuclear periphery. Thin section electron microscopy analysis revealed the presence of what appeared to be successive herniations of the nuclear envelope forming grape-like structures at primarily one site on the *nup145ΔN* nuclei. These successive herniations contained numerous NPC-like structures, correlating to the limited bright patches of antinucleoporin immunofluorescence signal. In some cases the successive herniations were small. Occasionally, however, multi-lobulated nuclei were seen. We suggest that the ultrastructural phenotype of *nup145ΔN* cells is due to a defective interaction of *nup145ΔN* NPCs with the surrounding pore membrane domain of the nuclear envelope. We have also analyzed the synthetic lethal phenotypes among GLFG nucleoporin mutant alleles, and found that strains harboring *nup116* and either *nup100* or *nup145* mutations were not viable. This, in combination with the morphological analysis, may reflect overlapping yet distinct roles for these three GLFG nucleoporins in NPC-nuclear envelope interactions.

THE pathway of nuclear pore complex (NPC)[1] biogenesis remains largely undefined. The large, modular NPC structure is embedded in a pore of ~90-nm diameter that joins the double lipid bilayers of the nuclear envelope and provides a portal for nucleocytoplasmic trafficking (for reviews see Miller et al., 1991; Forbes, 1992). The requisite steps for the fusion of the inner and outer nuclear membranes to form the pore, and for the coordinated assembly of the distinct substructures of an NPC have not been elucidated. The anchorage of the NPC in a pore is presumably mediated by interactions between individual NPC proteins (collectively referred to as nucleoporins) (Davis and Blobel, 1986) and integral membrane proteins of the pore membrane. The specific nucleoporins and integral pore membrane proteins that are responsible have not been identified. In fact, only a small fraction of the hundred or more nucleoporins that may comprise the estimated 10^8 D molecular mass of the NPC have been isolated and characterized (Reichelt et al., 1990; Rout and Blobel, 1993).

The seven nucleoporins that have been molecularly characterized to date in the yeast *Saccharomyces cerevisiae* can be classified into three families based on their primary structure. One family comprising Nup1p (Davis and Fink, 1990), Nup2p (Loeb et al., 1993), and Nsp1p (Nehrbass et al., 1990) contains multiple repeats in the central region of a degenerate sequence with a consensus core of XFXFG. These repeats are flanked by highly charged spacers. A second family comprising Nup100p (Wente et al., 1992), Nup116p, and Nup49p (Wente et al., 1992; Wimmer et al., 1992) lack repeats of this XFXFG motif and instead their amino-terminal regions have multiple tetrapeptide glycine–leucine–phenylalanine–glycine (GLFG) motifs separated by uncharged spacers. Finally, a yeast nucleoporin, Nic96p, that lacks both of these repetitive regions has also been reported (Grandi et al., 1993). Comparison between these yeast nucleoporins and those reported from rat (Starr et al., 1990; Sukegawa and Blobel, 1993; Radu et al., 1993) has revealed

Address all correspondence to Susan R. Wente, Department of Cell Biology and Physiology, Box 8228, Washington University School of Medicine, 660 S. Euclid Ave., St. Louis, MO 63110.

1. *Abbreviations used in this paper*: 5-FOA, 5-fluoroorotic acid; GLFG, glycine–leucine–phenylalanine–glycine; HA, epitope tag from the influenza hemagglutinin antigen; NPC, nuclear pore complex; SDM, synthetic minimal media.

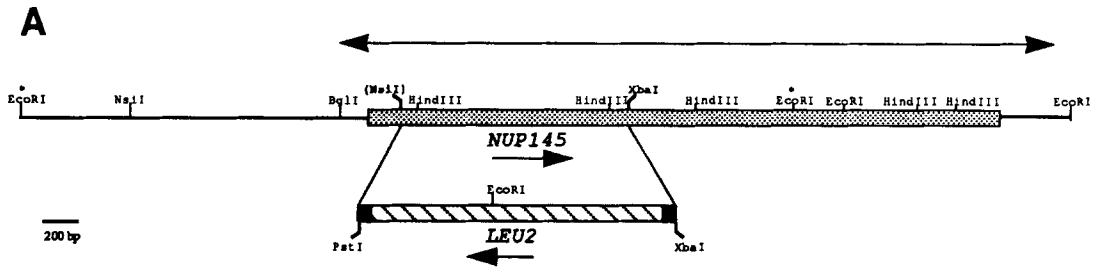
A
EcoRI
NsiI
BglI
(MseI)
HindIII
HindIII
XbaI
HindIII
EcoRI
EcoRI
HindIII
HindIII
EcoRI
NUP145
EcoRI
200 bp
LEU2
PstI
XbaI

B

some sequence similarities. However, functional homologues have not been identified.

If a yeast nucleoporin is directly involved in nucleocytoplasmic transport and/or NPC assembly, the phenotype of its mutant strain may reflect a perturbation of that particular NPC function. We previously characterized two distinct aberrations of NPC/nuclear envelope structure in a temperature-sensitive *nup116* null (Δ) strain (Wente and Blobel, 1993). First, at growth temperatures between 23 and 37°C, NPC-studded invaginations of inner nuclear membranes are present that have striking structural similarity to intranuclear annulate lamellae of other eukaryotic cells (for review see Kessel, 1983). Secondly, after growth at 37°C, nuclear envelope seals and subsequent membrane herniations form over the cytoplasmic face of *nup116*Δ NPCs coincident with the blockage of polyadenylated RNA export (Wente and Blobel, 1993). We proposed that the Nup116p-deficient NPCs are anchored less tightly to the surrounding pore membrane at 37°C, thus promoting the nuclear membrane fusion event that sealed the NPCs. Inner nuclear membrane invaginations and nuclear envelope sealing/herniations have not been previously reported in yeast cells. It is possible that these ultrastructural phenotypes of the yeast nuclear envelope may result in only particular nucleoporin mutant strains. Although nuclear import has been reported to be inhibited in genetic and biochemical studies of other NPC proteins (Finlay and Forbes, 1990; Nehrbass et al., 1990; Greber and Gerace, 1992; Mutvei et al., 1992; Schlenstedt et al., 1993), no coincident alterations in the ultrastructure of the nuclear envelopes have been described.

Five distinct GLFG nucleoporins have been identified based upon their cross-reactivity with mAb192 (Wente et al., 1992) and their coenrichment with isolated NPCs from yeast nuclei (Rout and Blobel, 1993). Although the genes encoding three members of the GLFG family have been isolated (*NUP116*, *NUP100*, and *NUP49*) (Wente et al., 1992; Wimmer et al., 1992), the genes encoding two other putative GLFG nucleoporins with apparent molecular masses of 65 and 54 kD (p65 and p54, respectively) have not been characterized. In this paper we describe a gene encoding the fourth member of the yeast GLFG family, *NUP145*, from which the p65 polypeptide is apparently generated by proteolysis. The amino-terminal half of Nup145p contains twelve GLFG motifs separated by uncharged spacers rich in glutamine, asparagine, serine, and threonine residues. This is followed by a region that is closely related to the carboxy-terminal sequences of both Nup100p and Nup116p. The deletion/disruption of this amino-terminal half of *NUP145* has only a slight effect on cell growth. However, by both immunofluorescence and thin section electron microscopy, this mutation results in striking, localized perturbations of nuclear envelope ultrastructure.

Materials and Methods

Isolation and Sequencing of NUP145

All DNA manipulations were conducted essentially as described by Sambrook et al. (1989). A yeast *S. cerevisiae* genomic λgt11 expression library from Clontech Laboratories, Inc. (YL1001b, lot 1108; Palo Alto, CA) was screened for mAb192 cross-reactive plaques as previously described (Wente et al., 1992). After screening over 1×10^7 recombinant phage two clones (Z1 and Z2) were obtained that did not encode Nup49p, Nup100p, Nup116p, Nup1p, or Nsp1p as determined by cross hybridization with respective DNA probes (Davis and Fink, 1990; Nehrbass et al., 1990; Wente et al., 1992). Restriction mapping revealed that the Z1 and Z2 clones were overlapping isolates of the same gene. λ DNA from plaque purified Z1 and Z2 clones was isolated by use of LambdaSorb (Promega Biotech, Madison, WI) and the ~4800-, 1600-, and 300-bp EcoRI fragments were individually ligated into pBS-KS+ (Stratagene Inc., La Jolla, CA) generating pSW69, pSW165, and pSW71, respectively. The resultant plasmids were transformed into DH5α bacterial cells (Bethesda Research Laboratories, Bethesda, MD) and cultured in Luria broth. The reported DNA sequence for both strands of the open reading frame (Fig. 1) was determined by the dideoxy chain termination method (Sanger et al., 1977) on denatured double stranded DNA (Haltiner et al., 1985) with [α-^{35}S]dATP (1,304 Ci/mmol; New England Nuclear, Boston, MA) and Sequenase Version 2.0 (United States Biochemicals Corp., Cleveland, OH). The unique oligonucleotide primers employed were synthesized by the Rockefeller University Biopolymers Facility (New York). A plasmid isolated by screening a YEp13 based yeast genomic library (Nasymth and Tatchell, 1980) with ^{32}P-labeled fragments from the Z1 clone was also sequenced (confirming the orientation of the EcoRI fragments). The DNA and predicted protein sequences were compared to the GenBank and EMBL data bases using the BLAST programs (Altschul et al., 1990).

Gene Disruption of NUP145 and Yeast Strain Analysis

To facilitate the construction of both the disrupted and epitope-tagged (see below) *NUP145* alleles, an NsiI restriction site was constructed at bp 2,386 of pSW69 (Fig. 1 *A*). The underlined nucleotide sequence in Fig. 1 *B* was changed in pSW69 with appropriate oligonucleotides and the polymerase chain reaction from AAC GCT AAT to AAT GCA TCT. This results in an NsiI site (Fig. 1 *A*; bold) and the mutation of amino acid residue 67 from N to S (Fig. 1 *B*; allele *nup145-2*) in pSW102.

Deletion and disruption of the amino-terminal half of *NUP145* (*nup145ΔN*) was accomplished by removal of a 1,452-bp NsiI/XbaI fragment from the middle of the open reading frame in pSW102 and coincident insertion of either the 2,008-bp NsiI/XbaI fragment from pJJ282 (yielding pSW133) or the 1078 bp NsiI/XbaI fragment of pJJ242 (yielding pSW115).

Figure 1. Sequence analysis of the *NUP145* locus and the encoded Nup145p protein. (*A*) The EcoRI fragments from the Z1 and Z2 λgt11 clones are displayed (the starred EcoRI sites indicate the insert contained in pSW69). The deletion/disruption that was made in the *NUP145* gene with a *LEU2* selectable marker is diagramed below, and the restriction sites used for the coincident gene deletion and marker insertion are bold faced. The sequence for the region covered by the double headed arrow is shown in *B*. The sites for the insertion of the *LEU2* marker (*NsiI* and *NbaI*) are designated in *B* by the open circles. (*B*) Nucleotide and predicted amino acid sequence of the *NUP145* locus. The predicted amino acid sequence (in single letter code) begins with the first AUG codon in the open reading frame and ends at the bold faced termination codon. The arrow marks the insertion site for the HA linker, at an NsiI site generated by mutagenesis of the underlined sequence to AAT GCA TCT. The GLFG repeat motifs are boxed, and the only two putative XFXFG motifs are underlined. The slash before amino acid 220 denotes the end of the GLFG region, and the slash at amino acid 592 marks the beginning of the putative carboxy-terminal region. The open circles note the restriction sites (*NsiI* and *XbaI* respectively) that were used to insert the *LEU2* marker in *A*. The shading over stretches of protein sequence before the second slash at amino acid 592 denote the four peptide sequences that were obtained from analysis of the p65 polypeptide. Protein sequence analysis of a different yeast NPC polypeptide, p80, yielded the three peptide sequences that are shaded in the carboxy-terminal half (after the second slash) (Rout, M., and G. Blobel, personal communication). The sequence data are available from EMBL/GenBank/DDBJ under accession number Z32672.

Table I. Yeast Strain Genotype and Construction

Strain	Genotype	Derivation
W303	Mata/Matα ade2-1/ade2-1 ura3-1/ura3-1 his3-11,15/his3-11,15 trp1-1/trp1-1 leu2-3,112/leu2-3,112 can1-100/can1-100	
W303a	Mata ade2-1 ura3-1 his3-11,15 trp1-1 leu2-3,112 can1-100	
SWY7	Mata/Mata ade2-1/ade2-1 ura3-1/ura3-1 his3-11,15/his3-11,15 trp1-1/trp1-1 leu2-3,112/leu2-3,112 can1-100/can1-100 nup100-3::TRP1/+	Integrative transformation of W303 with NcoI/NsiI fragments of pSW83
SWY9	Mata ade2-1 ura3-1 his3-11,15 trp1-1 leu2-3,112 can1-100 nup100-3::TRP1	Segregant from tetrad of sporulated SWY7
SWY68	Mata/Matα ade2-1/ade2-1 ura3-1/ura3-1 his3-11,15/his3-11,15 trp1-1/trp1-1 leu2-3,112/leu2-3,112 can1-100/can1-100 nup100-3::TRP1/+ nup116-5::HIS3/+	Cross of SWY9 and SWY27
SWY76	Mata/Matα ade2-1/ade2-1 ura3-1/ura3-1 his3-11,15/his3-11,15 trp1-1/trp1-1 leu2-3,112/leu2-3,112 can1-100/can1-100 nup145-1::URA3/+	Integrative transformation of W303 with EcoRI fragments of pSW115
SWY77	Mata ade2-1 ura3-1 his3-11,15 trp1-1 leu2-3,112 can1-100 nup145-1::URA3	Segregant from tetrad of sporulated SWY76
SWY78	Matα ade2-1 ura3-1 his3-11,15 trp1-1 leu2-3,112 can1-100 nup145-1::URA3	Segregant from tetrad of sporulated SWY76
SWY79	Mata ade2-1 ura3-1 his3-11,15 trp1-1 leu2-3,112 can1-100 nup145-1::URA3 pSW123(HIS3)	Transformation of SWY77 with pSW123
SWY120	Mata/Matα ade2-1/ade2-1 ura3-1/ura3-1 his3-11,15/his3-11,15 trp1-1/trp1-1 leu2-3,112/leu2-3,112 can1-100/can1-100 nup145-7::LEU2/+	Integrative transformation of W303 with EcoRI fragments of pSW133
SWY121	Matα ade2-1 ura3-1 his3-11,15 trp1-1 leu2-3,112 can1-100 nup145-7::LEU2	Segregant from tetrad of sporulated SWY120
SWY122	Mata ade2-1 ura3-1 his3-11,15 trp1-1 leu2-3,112 can1-100 nup145-7::LEU2	Segregant from tetrad of sporulated SWY120
SWY124	Mata/Matα ade2-1/ade2-1 ura3-1/ura3-1 his3-11,15/his3-11,15 trp1-1/trp1-1 leu2-3,112/leu2-3,112 can1-100/can1-100 nup145-7::LEU2/+ nup116-5::HIS3/+	Cross of SWY27 and SWY122
SWY125	Mata/Matα ade2-1/ade2-1 ura3-1/ura3-1 his3-11,15/his3-11,15 trp1-1/trp1-1 leu2-3,112/leu2-3,112 can1-100/can1-100 nup100-3::TRP1/+ nup145-7::LEU2/+	Cross of SWY9 and SWY12
SWY127	Mata ade2-1 ura3-1 his3-11,15 trp1-1 leu2-3,112 can1-100 nup116-5::HIS3 pSW131(URA3)	Segregant after transformation of SWY26 with pSW131
SWY130	Mata ade2-1 ura3-1 his3-11,15 trp1-1 leu2-3,112 can1-100 nup116-5::HIS3 nup100-3::TRP1 pSW131(URA3)	Segregant after transformation of SWY68 with pSW131
SWY133	Mata ade2-1 ura3-1 his3-11,15 trp1-1 leu2-3,112 can1-100 nup116-5::HIS3 nup145-7::LEU2 pSW131(URA3)	Segregant after transformation of SWY124 with pSW131
SWY136	Mata ade2-1 ura3-1 his3-11,15 trp1-1 leu2-3,112 can1-100 nup100-3::TRP1 nup145-7::LEU2 pSW132(URA3)	Segregant after transformation of SWY125 with pSW132
SWY137	Mata ade2-1 ura3-1 his3-11,15 trp1-1 leu2-3,112 can1-100 nup100-3::TRP1 nup145-7::LEU2	5-FOA selected from SWY136
SWY146	Mata ade2-1 ura3-1 his3-11,15 trp1-1 leu2-3,112 can1-100 pSW131(URA3)	Transformation of W303a with pSW131

Yeast transformations were by the lithium acetate method (Ito et al., 1983), and general genetic manipulations were conducted as described by Sherman et al. (1986). Strains SWY12, SWY19, SWY26, and SWY27 were from Wente et al. (1992) and Wente and Blobel (1993).

The inserted fragments encode the selectable markers *LEU2* or *URA3*, respectively (Jones and Prakash, 1990). The *nup145-7::LEU2* deletion/disruption is diagrammed in Fig. 1 *A* (*nup145-1::URA3* is analogous). Viable Leu$^+$ or Ura$^+$ transformants were selected after the integrative transformation (Rothstein, 1991) of the diploid strain W303 with the HindIII fragments of pSW133 or the EcoRI fragments of pSW115, respectively. Southern analysis identified the heterozygous diploid strains with the correct replacements of *NUP145*. Sporulation and dissection of either SWY120 or SWY76 yielded viable haploid strains lacking p65 (Table I).

The yeast strains for the synthetic lethal analysis were generated using the general genetic manipulations of Sherman et al. (1986). The *nup100-3::TRP1* allele was constructed using pSW83 (from insertion of the BamHI/EcoRI fragment of pJJ280 [Jones and Parkash, 1990] into BamHI/EcoRI digested pSW65 [Wente et al., 1992]). The *CEN/URA3* plasmids bearing *NUP116* (pSW131) or *NUP100* (pSW132) were constructed with appropriate fragments from pSW75 or pSW65, respectively, and pRS316 (Sikorski and Heiter, 1989; Wente et al., 1992). Yeast strains were grown in either YPD (1% yeast extract, 2% bactopeptone, 2% glucose) or synthetic minimal media (SDM) (Sherman et al., 1986) supplemented with appropriate amino acids and glucose. Selection against Ura$^+$ strains was done by culturing on solid synthetic media containing 1 mg/ml 5-fluoroorotic acid (5-FOA) (PCR Inc., Gainesville, FL) (Boeke et al., 1987). Yeast transformations were by the lithium acetate method (Ito et al., 1983).

Total yeast cell extracts were made as described by Yaffe and Schatz (1984) and electrophoresed in SDS-polyacrylamide gels (Laemmli, 1970) for electrophoretic transfer to nitrocellulose membranes. Blots were probed with a 1:5 dilution of mAb192 tissue culture supernant in TBST (10 mM Tris-HCl, pH 8.0, 150 mM NaCl, 0.05% Tween 20) plus 2% (wt/vol) nonfat dry milk overnight at 4°C. With TBST buffer washes between, antibody binding was detected by sequential incubations with affinity-purified anti-mouse IgG (Cappel Laboratories, Organon Teknika Corp., West Chester, PA) (diluted 1:500 in TBST, 1 h at room temperature), and then ^{125}I-protein A (100 mCi/ml; Dupont NEN, Wilmington, DE) (diluted 1:200 in TBST, 1 h, room temperature). The processed blots were dried and exposed for autoradiography on Kodak XAR film (Eastman Kodak Co., Rochester, NY).

Immunoelectron Microscopic Localization of Nup145p and Nup100p

An epitope-tagged allele of *NUP145* (*nup145-4::HA*) was constructed by

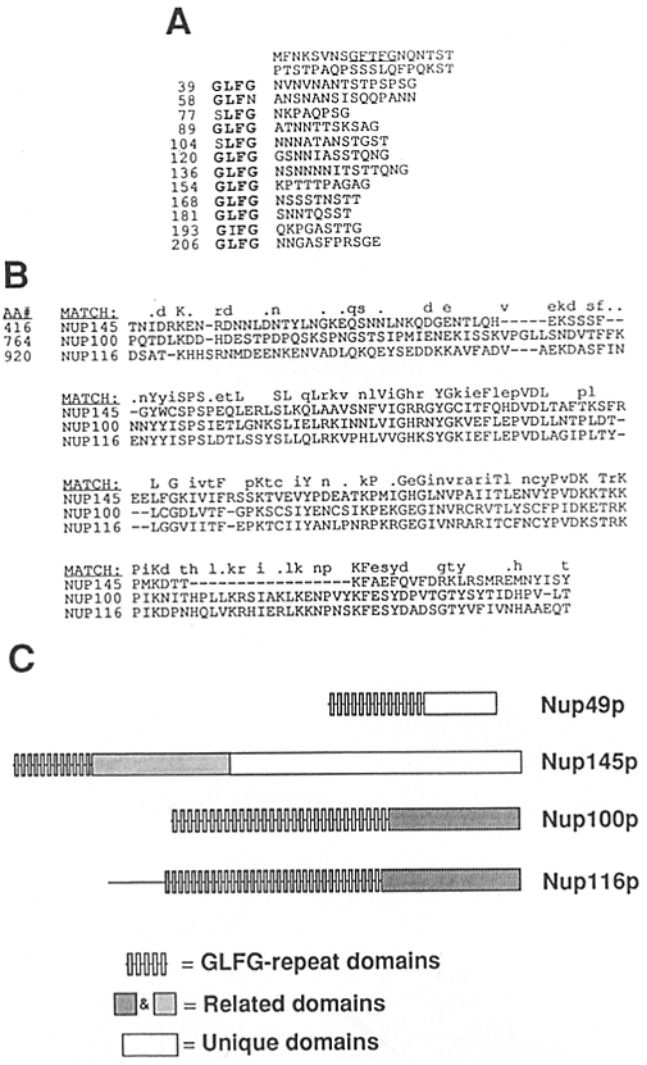

Figure 2. Yeast GLFG family of nucleoporins. (*A*) GLFG repeats in the amino-terminal region of Nup145p. The amino-terminal protein sequence of Nup145p has been aligned such that the consensus GLFG repeat is shown in the left column. Bold-faced type highlights the G, L, F, and G residues in these repeats. (*B*) Alignment of the Nup145p, Nup100p, and Nup116p related sequences. An ALIGN analysis (Dayhoff et al., 1983) between the last 175 amino acid residues of Nup100p and Nup116p to Nup145p sequence in the region following the GLFG repeats revealed a significant homology. The upper match line designates identical residues in all three (*capital letter*), identical residues in two of the three (*lower case letter*), and conserved residues in two of the three (.) proteins. (*C*) The yeast GLFG family of nucleoporins. The proposed domain structure for Nup49p, Nup145p, Nup100p, and Nup116p is shown. The amino-terminal regions of each are characterized by the GLFG motif where the number of individual boxes on the line reflects the number of repeat motifs in the respective domain. The homologous regions of Nup145p, Nup100p, and Nup116p are shaded (with the shaded area in Nup145p corresponding to the sequence found between the slashes in Fig. 1 *B*), whereas the unique Nup49p and Nup145p carboxy-terminal regions are unshaded.

ligating an excess of the FLUI/FLU2 linker from Wente et al. (1992) into the new NsiI site in pSW102. The in-frame insertion of a tandem repeat of this linker effectively results in a 24-residue insertion between amino acid 67 (N) and 68 (S) in pSW118 of [TPTDVPDYATANTPTDVPDYATAS] (HA epitopes underlined, confirmed by DNA sequencing). This epitope-tagged gene was subcloned into pRS313 (*CEN* and *HIS3*) (Sikorski and Hieter, 1989) via the EcoRI sites (starred in Fig. 1 *A*), generating pSW123 and enabling expression of the first ~100 kD of Nup145p. Expression in the *nup145ΔN* background was obtained by transforming pSW123 into SWY77 (yielding SWY79). For immunolocalization of Nup100p or Nup145p, spheroplasts from SWY19 (Wente et al., 1992) or SWY79 were processed as previously described (Wente et al., 1992). The thin sections were incubated with tissue culture supernant of the monoclonal antibody 12CA5 (Berkeley Antibody Co., Richmond, CA) diluted 1:2 in 1% BSA/0.2% fish gelatin/PBS, and 10-nm colloidal gold coated with goat anti-mouse antibody (Amersham Corp., Arlington Heights, IL). Photographs recorded with Kodak EM Film of uranyl acetate-stained specimens were obtained by visualization with a JEOL 100CX electron microscope (JEOL USA, Inc., Peabody, MA) at 80 kV.

Immunofluorescence and Electron Microscopy for Morphological Analysis

Early log phase yeast cells were prepared for immunofluorescence microscopy with the modified method of Kilmartin and Adams (1984) exactly as described in Wente et al. (1992). The binding of mAb192 or mAb414 was visualized with affinity-purified, FITC-conjugated, goat anti-mouse IgG (Cappel Lab.) at a 1:50 dilution. Photographs were taken for the same exposure time with a 100× objective on a Zeiss Axiophot microscope with Kodak T-MAX400 film processed at 1600 ASA.

Preservation of both protein and membrane structures in the electron microscopy studies was obtained using the protocols described in Wente and Blobel (1993). Briefly, a pellet of 10^8 early log phase cells was resuspended in 40 mM K_2HPO_4-KH_2PO_4, pH 6.5, 0.5 mM $MgCl_2$, 2% glutaraldehyde (BDH; Gallard Schlesinger Chem., Carle Place, NY), 2% formaldehyde (Fluka Chemical Corp., Ronkonkoma, NY), and incubated on ice for 30 min. After cell wall digestion and osmium postfixation (Byers and Goetsch, 1991), the samples were embedded in EPON. Thin sections collected on nickel grids coated with formvar, stabilized with carbon, were contrasted by staining with uranyl acetate and Reynold's lead. Specimens were visualized as described above.

Results

Isolation of the Gene Encoding the GLFG Nucleoporin Nup145p

We previously reported the isolation and characterization of the genes encoding three members of the GLFG family; *NUP116*, *NUP100*, and *NUP49* (Wente et al., 1992). To isolate genes encoding novel GLFG nucleoporins, we exhaustively screened a yeast *S. cerevisiae* genomic λgt11 expression library for mAb192 cross reactive plaques. The GLFG repetitive motif is the likely epitope for recognition by mAb192 (Wente et al., 1992). In this report we describe overlapping positive clones, Z1 and Z2, that were distinct from *NUP49*, *NUP100*, and *NUP116*. Bacterial cell extracts from Z1 and Z2 lysogenic strains were analyzed by immunoblotting and although they did not encode a *lacZ* fusion protein, a mAb192 cross-reactive polypeptide of greater than 100 kD was expressed and readily proteolyzed to an ~65-kD product (data not shown) (confirmed by DNA and protein sequencing, see below). The complete DNA sequence of the EcoRI fragments from the λ clones was determined (Fig. 1). The nucleotide sequence for the region covered by the horizontal arrow in Fig. 1 *A* and the predicted amino acid sequence of the open reading frame found therein are presented in Fig. 1 *B*. Beginning at bp 2,191, a gene that was capable of encoding a polypeptide of 1314 amino acids with a predicted molecular mass of 145.3 kD was found. This open reading frame utilized the first methionine (with the next at amino acid 239) and was in general agreement with the requirements for transcriptional and translational signals. The gene has been designated *NUP145* (nucleoporin

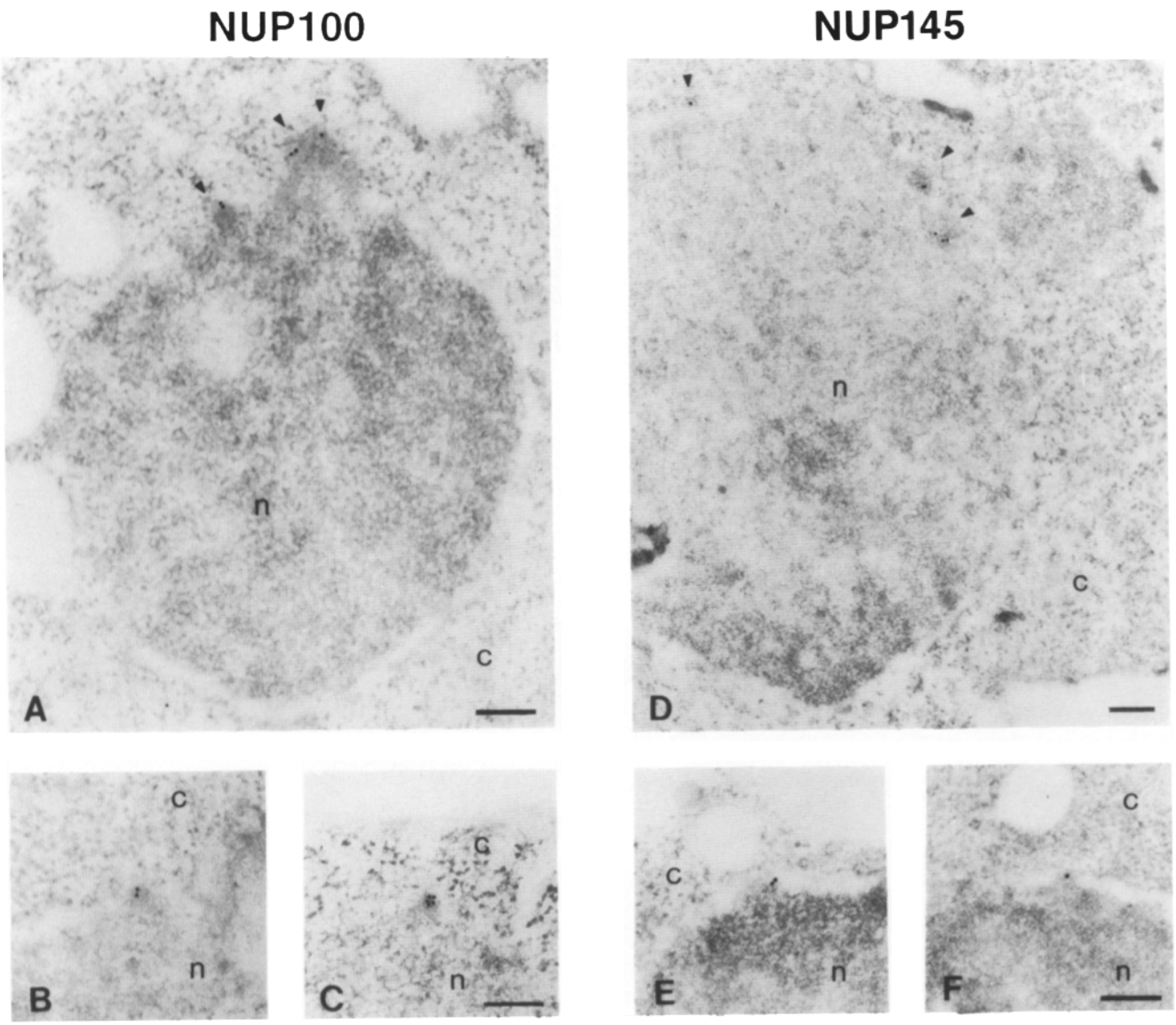

Figure 3. Epitope-tagged Nup145p and Nup100p are localized at yeast nuclear pore complexes. Immunolabeling of thin sections from LR White-embedded yeast spheroplasts of the haploid strains SWY19 (HA-tagged Nup100p; *A–C*) and SWY79 (HA-tagged Nup145p; *D–F*) was performed as described in Materials and Methods. The HA-tagged Nup145p was evaluated from a construct expressing the amino-terminal-tagged first ~100 kD of Nup145p in a *nup145ΔN* strain (pSW123). The binding of the monoclonal antibody 12CA5 which recognizes the epitope tag was visualized by colloidal gold particles (10 nm) coated with a goat anti-mouse antibody. The micrographs in *A* and *D* show thin sections of entire nuclei, whereas those in *B*, *C*, *E*, and *F* show representative labeling of NPCs. The nucleoplasm (*n*) and cytoplasm (*c*) are separated by a clear area between the two nuclear membranes. The NPCs appear as protein dense patches along the nuclear envelope. In *A* and *D* the gold particles that label such NPCs are indicated by arrows. Quantitation of the gold particles in representative cell thin sections is presented in Table II. Bars, 0.2 μm.

Table II. Distribution of 12CA5 Antibody Labeling in Immunoelectron Microscopy Experiments

	Number of gold particles			Density (gold particles/μm²)		
	Nucleoplasm	NPC	Cytoplasm	Nucleoplasm	NPC*	Cytoplasm
Nup100p-HA	2	43	25	0.2	5.8*	0.4
Nup145p-HA	1	48	35	0.1	4.3*	0.3

The number and location of 10-nm gold particles in 12 or 18 cell thin sections of postembedded haploid spheroplasts, representing the binding of the mAb 12CA5 in a strain expressing epitope-tagged Nup100p or Nup145p respectively, are shown. The density of gold particle labeling was calculated using the average area of the nucleoplasm, nuclear envelope, and cytoplasm in thin sections of five typical cells.

* These values are an underestimate as the area of the entire nuclear envelope was used to calculate the density at the NPCs (the number of pore complexes per section was variable).

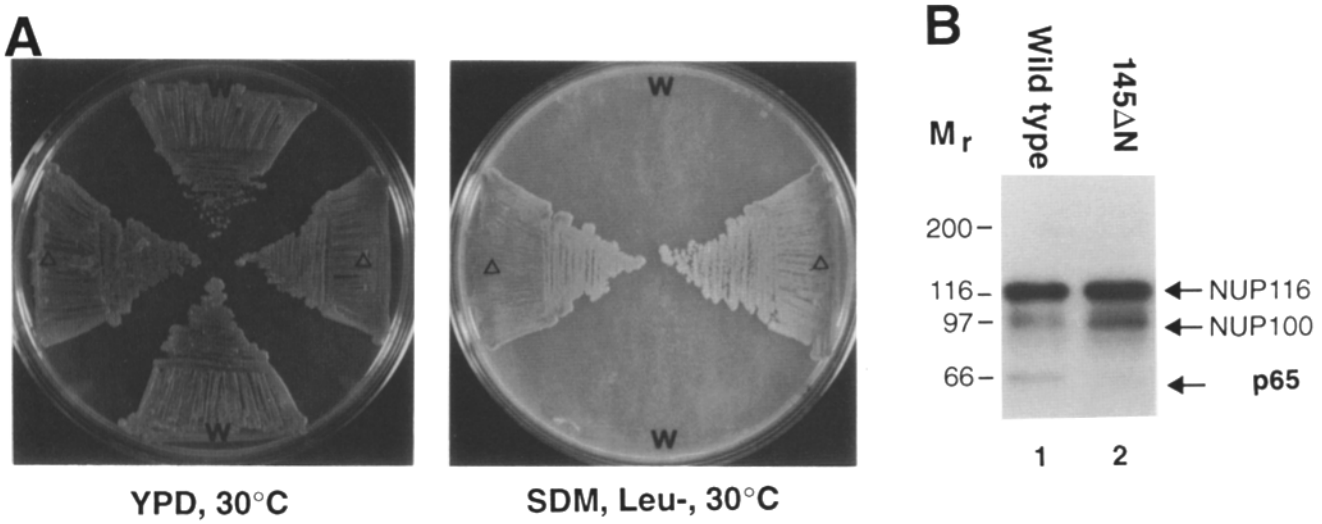

C. *nup145ΔN* Growth Parameters

Growth Temperature	Doubling Time (h) *nup145ΔN*	Doubling Time (h) wild type	Ratio 145ΔN/wt
37°C	2.8	2.0	1.4
30°C	2.5	1.8	1.4
23°C	3.0	2.4	1.25
17°C	5.2	4.8	1.1

Figure 4. The amino-terminal half of *NUP145* is not essential for cell viability. (*A*) Deletion/disruption of *NUP145* results in a viable haploid strain. Cells isolated from each single tetrad of a sporulated diploid heterozygous for the *nup145ΔN* allele (SWY120) were streaked to both a YPD plate and a SDM, Leu$^-$ plate and grown for 2 d at 30°C. Growth of the two *nup145ΔN* haploid segregants (designated Δ, strains SWY121 and SWY122 in Table I) on the SDM, Leu$^-$ plate reflects the presence of the *LEU2* selectable marker that was inserted into the *NUP145* locus (Fig. 1 *A*). The *nup145ΔN* strains were also shown by Southern analysis to have the gene replacement and by immunoblotting (see Fig. 4 *B*) to lack the p65 polypeptide. The strains designated *w* were wild type by the same criteria. (*B*) Immunoblots with mAb192 of proteins from disrupted haploid strains. Proteins from total cell extracts of haploid yeast strains were separated by electrophoresis on a 7% SDS–polyacrylamide gel, transferred to nitrocellulose, and processed as described in Materials and Methods. (Lane *1*) *Wild type* (W303a); (lane *2*) *145ΔN* (SWY122). Molecular mass markers are indicated at the left in kD. (*C*) Doubling times for *nup145ΔN* versus wild-type cells. Doubling times in YPD liquid media were calculated by directly monitoring cell number/volume during logarithmic phase growth at the designated growth temperature. *Wild type* (W303a); *145ΔN* (SWY122).

with a calculated molecular mass of 145 kD) (Davis and Fink, 1990; Wente et al., 1992).

Analysis of the primary amino acid sequence revealed that Nup145p contains at least three distinct structural regions; the region comprised by the first 219 amino acid residues possesses no acidic residues and only six well spaced lysine (K) residues, whereas the remainder contains a mixture of charged residues. In particular, the amino-terminal region also has multiple repeats of tetrapeptide GLFG motifs (boxed in Fig. 1 *B* and aligned in Fig. 2 *A*). The spacer sequences between the GLFG repeats are noticeably rich in asparagine (*N*), glutamine (*Q*), serine (*S*), and threonine (*T*) residues (Fig. 2 *A*). These sequence features are consistent with our previous definition of a GLFG domain in the amino-terminal regions of Nup49p, Nup100p, and Nup116p (Wente et al., 1992). The two underlined pentameric motifs in Fig. 1 *B* resemble the XFXFG motifs and may allow recognition by the polyspecific antinucleoporins mAb414 and mAb350 (Davis and Fink, 1990; Wente et al., 1992; Rout and Blobel, 1993; S. R. Wente, unpublished data).

We propose that Nup145p is a fourth member of the GLFG family of yeast nucleoporins (Fig. 2 *C*). However, a GLFG polypeptide of this apparent molecular mass (greater than 120 kD) had not been observed when yeast cell fractions were immunoblotted with mAb192 (Wente et al., 1992; Rout and Blobel, 1993). The putative GLFG nucleoporin with an apparent molecular mass of 65 kD (p65) has been purified from an enriched yeast NPC fraction using HPLC and SDS-hydroxylapatite chromatography (Rout and Blobel, 1993; Wozniak et al., 1994). Four internal peptide sequences obtained from p65 were found within the amino-terminal half of the predicted *NUP145* gene product (before the second slash in Fig. 1 *B*). Thus, the p65 GLFG nucleoporin identified in yeast cell fractionation is a proteolytic product derived from the amino-terminal half of Nup145p. That Nup145p is cleaved into at least two discrete fragments has been confirmed by protein sequence analysis of a novel 80-kD polypeptide (p80) that cofractionates with highly enriched yeast NPCs (yielding the three peptide sequences found in the carboxy-terminal half of Fig. 1 *B*; Rout, M., and G. Blobel, personal communication). To determine any possible physiological relevance of this cleavage will require further investigation. At least one more novel yeast nucleoporin with a GLFG region and an apparent molecular mass of 54 kD remains to be characterized (Wente et al., 1992; Rout and Blobel, 1993).

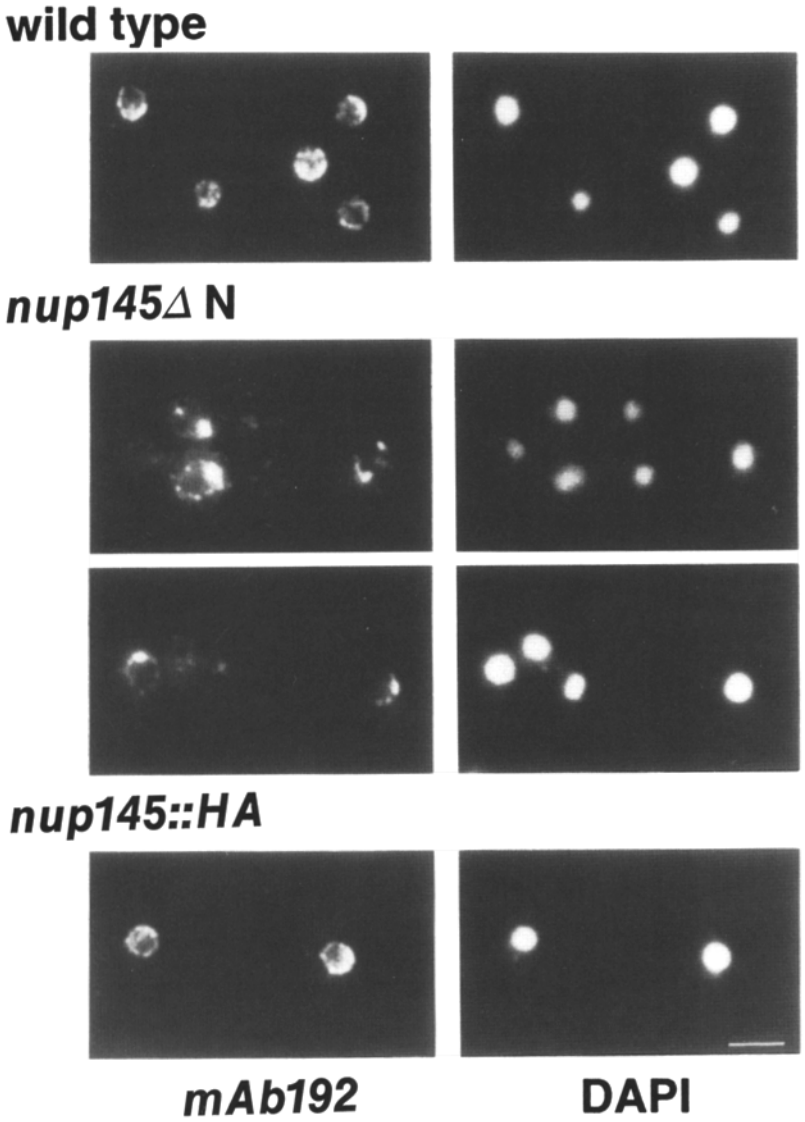

Figure 5. The staining pattern by indirect immunofluorescence microscopy with an antinucleoporin antibody is different in *nup145ΔN* versus wild-type cells. Formaldehyde/methanol-fixed yeast cells were incubated with mAb192 and binding was detected with an FITC-conjugated goat anti-mouse IgG. In wild-type yeast cells (upper left, W303a), antinucleoporin staining with mAb192 is nuclear, distinctly punctate, and localized to the nuclear periphery. In contrast, the staining in *nup145ΔN* cells (SWY122) is concentrated in only one or two areas of the nuclear periphery (*middle left*). The expression of the HA-tagged Nup145p in the mutant strain background (SWY79) restores the signal to the wild-type pattern (*lower left*). The coincident DAPI staining is also shown (*right*). Bar, 3 μm.

Related Regions of Nup145p, Nup116p, and Nup100p

The first acidic amino acid residue (220 glutamic acid (E) after the slash in Fig. 1 *B*) denotes the beginning of a second region in the amino terminal half of Nup145p. In our previous study (Wente et al., 1992), we noted considerable similarity between the carboxy-terminal regions of Nup100p and Nup116p. Likewise, alignment of 175 residues from the shaded area of Nup145p in Fig. 2 *C* with the carboxy-terminal region of either Nup100p or Nup116p gave an overall similarity index of 55% (36% conserved/29% identical or 24% conserved/31% identical, respectively) (Fig. 2 *B*). When only the carboxy-terminal regions of Nup100p and Nup116p are aligned their similarity index is greater (78%, Wente et al., 1992). The overall predicted isoelectric points for Nup100p, Nup116p, and the amino-terminal half of Nup145p are basic and nearly identical (9.38, 9.32, and 9.32, respectively). However, the predicted isoelectric point for the full-length Nup145p is 5.45 reflecting the highly acidic contribution of the remaining carboxy-terminal half. The isoelectric point calculated for Nup49p is also acidic (5.94) (Wente et al., 1992), but comparison of the carboxy-terminal half of Nup145p to Nup49p and to the protein sequences in the GenBank and EMBL data bases failed to detect any notable similarities. The second slash in Fig. 1 *B* (before amino acid residue 592 asparagine [N] indicates the point at which the similarities to Nup100p and Nup116p end and the novel region of Nup145p begins (unshaded in Fig. 2 *C*).

The flanking sequences of *NUP145* lack the histidine tRNA gene and Tyl-delta element that are found in the 3′ noncoding sequences of both *NUP100* and *NUP116* (Wente et al., 1992). Overall, Nup100p and Nup116p are more closely related to each other than either is to Nup145p, as indicated by the slightly different shading of the related regions in Fig. 2 *C*. This limited similarity may reflect shared, yet specialized, functions for Nup145p and the Nup100p/Nup116p pair. In contrast, the conserved GLFG region and the region aligned in Fig. 2 *B* may serve common functions; e.g., interactions with other nucleoporins, with integral membrane proteins of the pore membrane, or with transport substrates for nucleocytoplasmic traffic.

Immunolocalization of Nup145p and Nup100p to the NPC

Nup145p and Nup100p are similar to two other GLFG nucleoporins that have been definitively localized to the NPC by immunoelectron microscopy with monospecific antibodies (Nup49p, Wente et al., 1992; Nup116p, Wente and Blobel, 1993). Both Nup100p and the proteolytic products of Nup145p (p65 and p80) coenrich with isolated NPCs (Rout and Blobel, 1993; Rout, M., and G. Blobel, personal communication). To definitively determine whether these proteins are indeed nucleoporins, we performed immunoelectron microscopy. An in-frame insertion in the *NUP145* gene of a sequence encoding two tandem repeats of a unique nine-amino acid epitope derived from the influenza hemagglutinin antigen (HA) (Wilson et al., 1984) was made at the point designated by the arrow in Fig. 1 *B*. This epitope-tagged gene (*nup145-4::HA*) was expressed under control of its endogenous promoter on a *CEN/HIS3* plasmid in a *nup145* mutant (ΔN) strain background (SWY79). In a similar fashion, a HA-tagged *nup100* gene constructed in our previous studies (Wente et al., 1992) was expressed in a *nup100Δ* strain background (SWY19). The binding of the monoclonal antibody 12CA5 directed specifically against the HA epitope to thin sections of postembedded spheroplasts from SWY79 or SWY19 was visualized by the presence of 10-nm colloidal gold particles coated with anti-mouse antibody. In the micrographs of Fig. 3 showing an entire nucleus (*A* and *D*) or higher magnification views of labeled NPCs (*B*/*C* and *E*/*F*, respectively), Nup100p and Nup145p were found along the nuclear envelope and coincident with protein densities typical of NPCs. The position of gold particles in multiple cell sections and the relative gold particle density (Table II) were similar to that observed in the immunolocalization of HA-tagged Nup49p (Wente et al., 1992) and HA-tagged Nup116p (Wente and Blobel, 1993). Thus, Nup145p and Nup100p are yeast nucleoporins. The precise localization of the GLFG nucleoporins to the substructures of an NPC (i.e., rings, spokes, basket, fibrils, etc.) will only be accomplished when the resolution of current yeast NPC immunoelectron microscopy technology improves.

Deletion/Disruption of the Amino-terminal Half of Nup145p Does Not Compromise Cell Viability

From the immunological and biochemical analysis of nucleoporin fractions (Wente et al., 1992; Rout and Blobel, 1993) we initially predicted that *NUP145* encoded the p65 GLFG nucleoporin. The sequence analysis (Figs. 1 and 2) revealed clear homologies between the amino-terminal p65 portion and the other GLFG nucleoporins, whereas the carboxy-terminal p80 portion had no similarities with any other known proteins. Therefore, to begin analyzing the function of Nup145p, only the amino-terminal half of Nup145p was targeted for disruption and the phenotype of the resulting mutant strain was assessed (*nup145ΔN*). Fig. 1 *A* displays one of the deletion/disruption constructs that was employed. The sporulation and dissection of the heterozygous *nup145-7::LEU2* diploid strain (SWY120) resulted in the recovery of four viable spores (Fig. 4 A, *left plate*). The same four strains from a single tetrad were streaked on selective media (Fig. 4 *A*, *right plate*) and analyzed by Southern blotting (data not shown) to verify a 2:2 segregation of the *LEU2* marker with the *nup145ΔN* mutation. As shown in Fig. 4 *B* by immunoblotting, the absence in *nup145ΔN* cells of the mAb192 cross reactive band at about the apparent molecular mass of the p65 protoelytic product (*arrow*) confirmed that this part of the Nup145p protein was absent and not required for cell growth. The growth rates in liquid culture of wild-type versus *nup145ΔN* cells were compared at a range of temperatures (Fig. 4 *C*). Consistently, at the temperatures tested, the doubling time for the *nup145ΔN* cells was only slightly longer than that of the wild-type counterparts. It is possible that the *nup145ΔN* mutation may allow transcriptional reinitiation in the intact carboxy-terminal half, and expression of the remaining part of the *NUP145* gene. Further deletion/disruption analysis of *NUP145* will be required to directly evaluate any requirement for the carboxy-terminal region.

Perturbations of Nuclear Envelope Structure in nup145ΔN Cells

In wild-type yeast cells, immunofluorescence staining with a polyspecific monoclonal antibody recognizing the GLFG nucleoporin family (mAb192) (Wente et al., 1992) was punctate and localized all around the nuclear periphery (Fig. 5, *top left*). In contrast, in at least 75% of the *nup145ΔN* cells most of the mAb192 immunofluorescence signal was present in only one or two places at the nuclear periphery with the punctate staining intensity around the rest of the nuclear perimeter coincidentally reduced. A similar staining pattern was observed when two other polyspecific monoclonal antibodies that preferentially recognize the XFXFG family of nucleoporins were used; mAb414 and mAb350 (Davis and Blobel, 1986; Davis and Fink, 1990) (data not shown). The expression of the HA-tagged *nup145* gene in the mutant strain background restored the wild-type immunofluorescence pattern (Fig. 5, *lower left*).

To investigate the ultrastructural basis of the altered immunofluorescence signal, the *nup145ΔN* cells were examined by thin section electron microscopy. NPCs were present (Fig. 6 *A*, *closed arrowheads*), together with clusters of unusual grape-like extrusions of the nuclear envelope that contain NPC-like structures (Fig. 6, *A* and *B*, *arrow*). Such clusters were not observed in wild-type yeast cells (Fig. 6 *E*). At higher magnification (Fig. 6 *C*) the grape-like clusters appeared to be derived from a network of successive, and interconnected, herniations of the nuclear envelope. Individual herniations seemed to be linked by NPC-like structures (densely staining). Multiple NPC-like structures on individual herniations (Fig. 6 *A*) were also present, thus generating multiple branch points and the clustering appearance. The entire grape-like cluster often resides under a protrusion of the outer nuclear membrane. Such clusters of successive herniations with numerous NPC-like structures were present at all tested growth temperatures for *nup145ΔN* cells (for example at 17°C in Fig. 6 *F*). These clusters most likely correspond to the antinucleoporin immunofluorescence signal in a few concentrated areas of the nuclear envelope (Fig. 5).

The NPC-like structures seemed to constrict the size of the branch points between most individual herniations to ~100 nm. However, occasionally the size of the membrane herniations could be very large such that the nuclei appeared lobulated (Fig. 6, *A* and *B*, *open arrowheads*). The particular cell

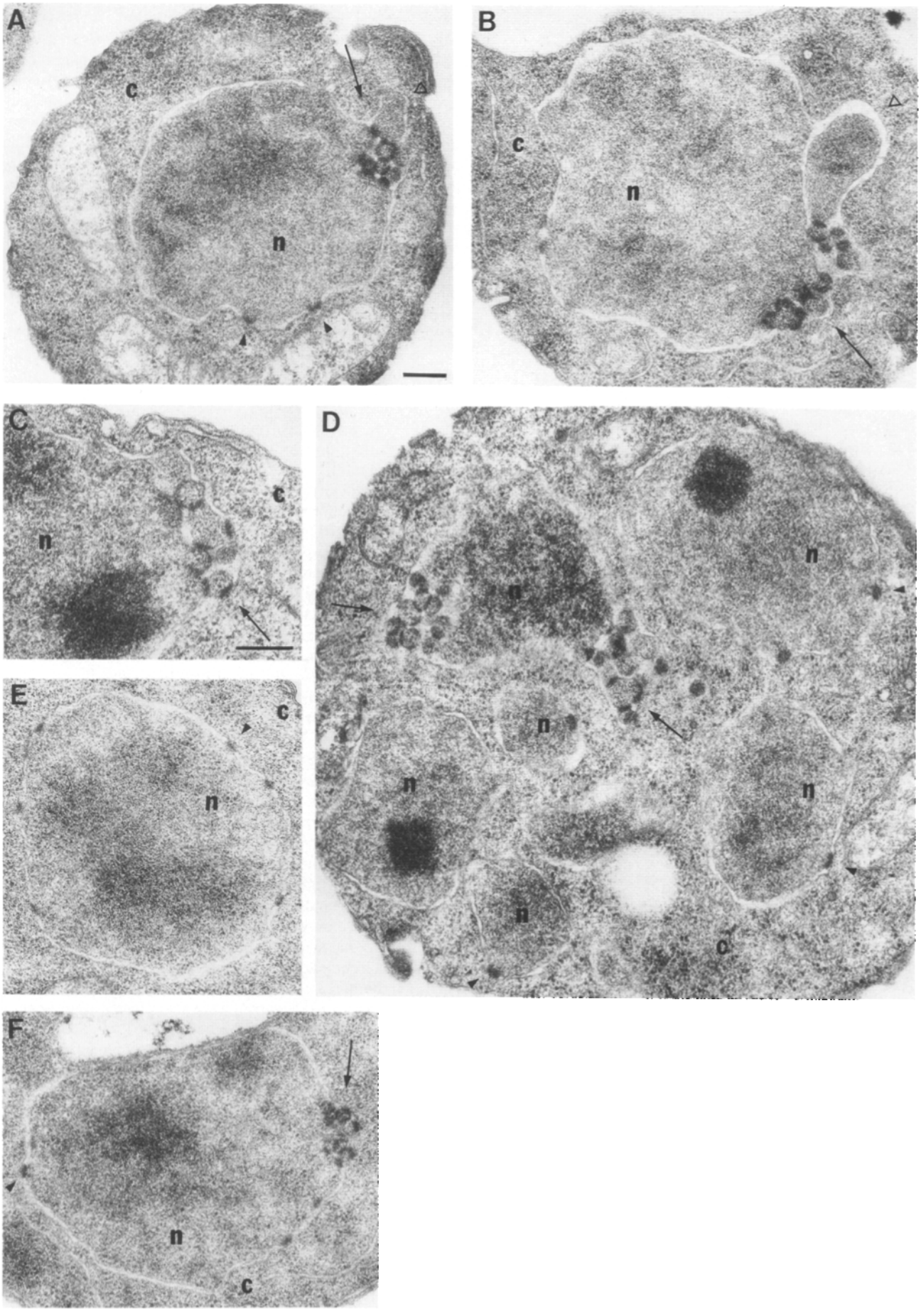
A
c
n
B
c
n
C
c
n
D
n
n
n
n
n
n
c
E
c
n
F
n
c

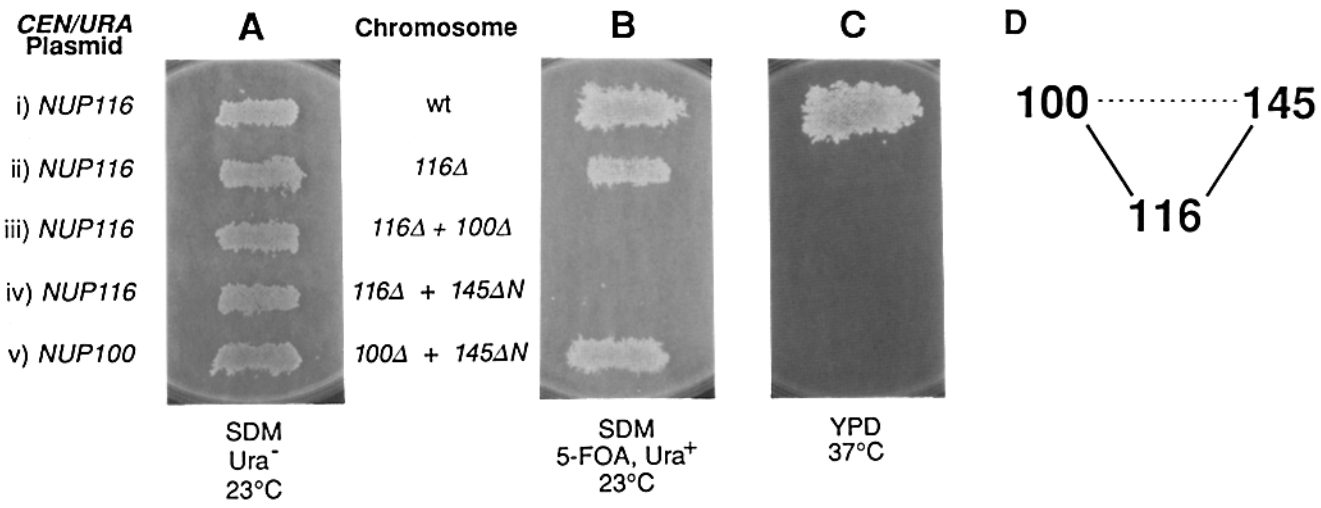

Figure 7. Synthetic lethal analysis among the mutant alleles for *NUP116*, *NUP100*, and *NUP145*. The haploid strains patched on the SDM, Ura⁻ plate bear the designated chromosomal mutation (null = Δ; amino disruption/deletion = ΔN) alleles and a *CEN/URA3* plasmid with a wild-type copy of the designated nucleoporin gene (*i*, SWY146; *ii*, SWY127; *iii*, SWY130; *iv*, SWY133; *v*, SWY136; as described in Materials and Methods and Table I). After growth on the SDM, Ura⁻ plate in *A* for 5 d at 23°C, the cells were replica plated to SDM, Ura⁺ plates containing 1 mg/ml 5-FOA (*B*). After 5 d at 23°C, the cells from the plate in *B* were finally replica plated to YPD media and tested for growth at 37°C for 3 d (*C*). The diagram in *D* reflects the lethal phenotypes of the *116Δ/100Δ* and *116Δ/145ΔN* combinations (*solid lines*) and the viable, although temperature-sensitive, phenotype of the *100Δ/145ΔN* strain (*dashed line*).

section in Fig. 6 *D* bisects at least six such nuclear (*n*) lobules (some large with apparently individual NPCs [arrowhead] and some with successive herniations containing numerous NPC-like structures [arrow]). The content, particularly of the large herniations, appeared to be indistinguishable from the nucleoplasm (Fig. 6, *A–D*).

Synthetic Lethal Analysis Among the Related Nup145p, Nup116p, and Nup100p GLFG Nucleoporins

Nup116p-deficient cells grow very slowly and are temperature sensitive (Wente et al., 1992), whereas the lack of either Nup100p (Wente et al., 1992) or at least the amino-terminal half of Nup145p (Fig. 4) has only a slight effect on cell doubling. Because of their primary structure similarities (Fig. 2, *B* and *C*), the viability of the single *nup116Δ*, *nup100Δ*, and *nup145ΔN* mutations may be a reflection of the proteins' functional redundancy in the NPC. To test for possible functional overlaps among these GLFG nucleoporins, a series of genetic experiments was conducted. The phenotypes for three pair-wise combinations of the mutant alleles were tested in haploid strains bearing the designated chromosomal disruptions and a plasmid-borne (*CEN/URA3*) wild-type gene (Fig. 7). The assay for cell viability is based on the toxicity of the drug 5-FOA in a *URA3* background (Boeke et al., 1987). Only strains that can lose the *URA3* plasmid and survive without the wild-type nucleoporin gene will be viable on 5-FOA media. The wild-type strain is viable under all conditions (Fig. 7 *i*, *A–C*), and as expected the absence of *NUP116* (Fig. 7 *ii*) resulted in a temperature-sensitive strain (*B* to *C*). The strain with both the *nup100Δ* and the *nup145ΔN* mutations (Fig. 7 *v*, *B* to *C*) was also a temperature-sensitive strain. Strains harboring *nup116Δ* and either *nup100Δ* (Fig. 7 *iii*) or *nup145ΔN* (Fig. 7 *iv*) were not viable at 23°C. Based upon these synthetic lethal results, the diagram in Fig. 7 *D* and drawn to highlight the interactions that may exist between Nup116p, Nup100p, and Nup145p. The solid lines represent the requirement of both gene products for cell viability and a possible functional overlap and/or structural interaction. In contrast, connection by the dashed line reflects a conditionally viable phenotype and only partially overlapping roles.

Nuclear Envelope Ultrastructure in nup100Δ/nup145ΔN Cells

The deletion of *NUP100* alone has no discernable effect on cell viability or nuclear envelope ultrastructure (Wente et al., 1992). However, its absence in combination with the *nup145ΔN* allele significantly compromised cell viability at 37°C (Fig. 7 *v*). To determine whether the *nup100Δ/nup145ΔN* cells displayed the ultrastructural phenotype of either single mutant or a novel aberration, we examined the *nup100Δ/nup145ΔN* cells by thin section electron microscopy. After growth at 23°C, structures with striking similarity to the *nup145ΔN* morphology were present: clusters of successive herniations with numerous NPC-like structures (Fig. 8,

Figure 6. Electron microscopic analysis of the nuclear envelope in *nup145ΔN* cells. The *nup145ΔN* (SWY122) (*A–D*, and *F*) or wild-type cells (W303a) (*E*) were grown to early logarithmic phase at 30 (*A–E*) or 17°C (*F*) and then processed for optimal visualization of protein and membrane structures (see Materials and Methods). The micrographs show examples of apparently intact NPCs (*closed arrowhead*), the grape-like extrusions of nuclear envelope that contain NPC-like structures (*arrow*), and lobulated nuclear herniations (*open arrowhead*). *n*, nucleus; *c*, cytoplasm. Bars: (*A*, *B*, and *D–F*) 0.25 μm; (*C*) 0.25 μm.

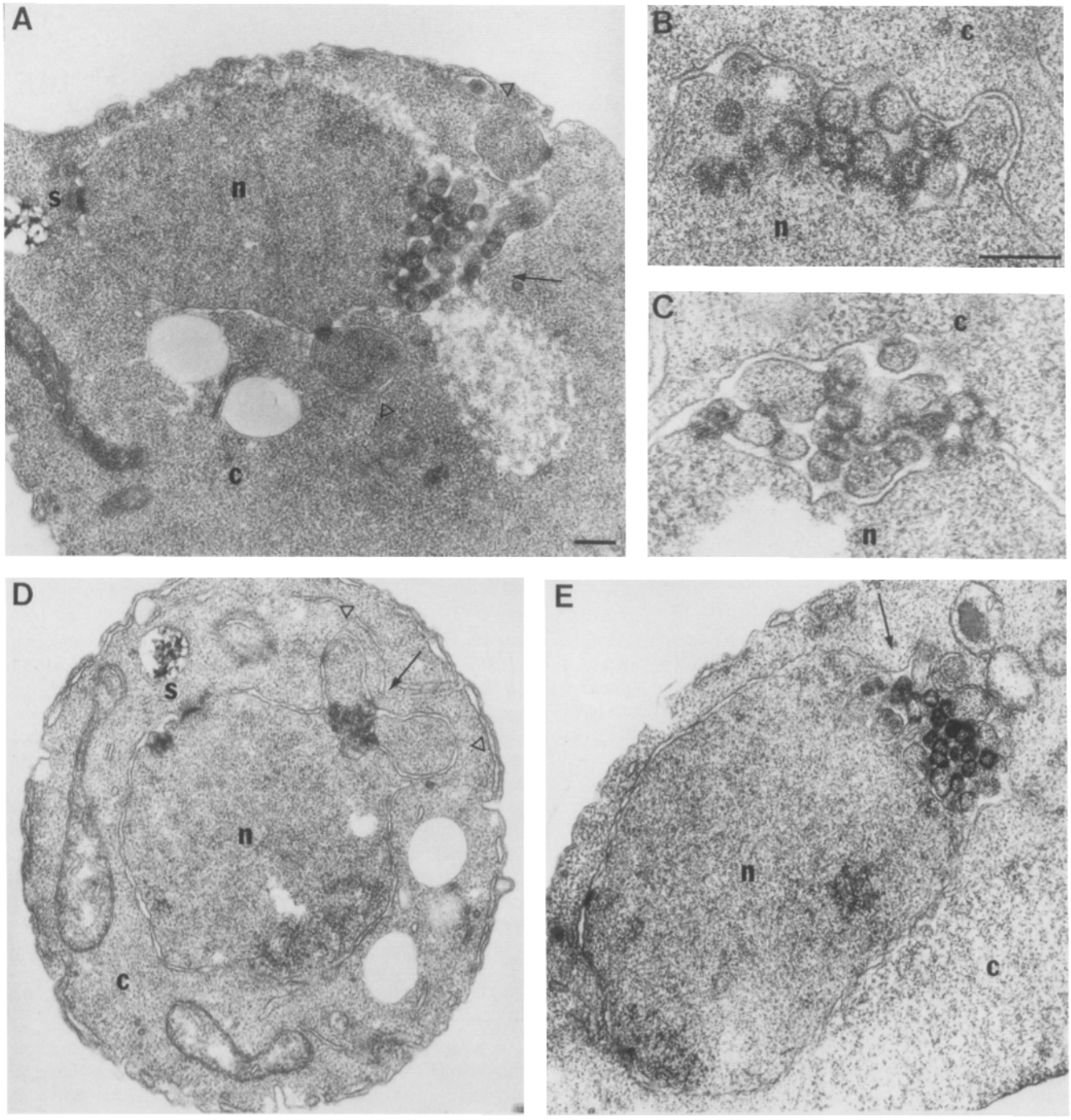

Figure 8. Thin section electron microscopic analysis of *nup100Δ/nup145ΔN* cells. The *nup100Δ/nup145ΔN* cells (SWY137) were grown to early logarithmic phase at 23°C (*A–D*) and then shifted to 37°C for 6 h (*E*) before fixation, embedding, and staining for optimal visualization of protein and membrane structures. The grape-like clusters of NPC/nuclear envelope structures (*arrow*) and nuclear lobules (*open arrowhead*) are shown in multiple different cell sections. *n*, nucleus; *c*, cytoplasm; *s*, spindle pole body. Bars: (*A*, *D*, and *E*) 0.25 μm; (*B* and *C*) 0.25 μm.

A–C). Pore clustering was more pronounced than in the *nup145ΔN* strain. Lobulations of the nucleus (i.e., Fig. 8 *D*, *open arrowhead*) were also observed. When these temperature-sensitive *nup100Δ/nup145ΔN* cells were grown at 37°C for 6 h, no changes in the structure of the clusters were detected (Fig. 8 *E*). The primary cause of cell death at the nonpermissive temperature may be unrelated to the clustering phenotype and will require further study. When multiple sections were examined from both *nup145ΔN* and *nup100Δ/nup145ΔN* cells, the location of the clusters appeared random with respect to the nucleolus or the spindle pole body (Fig. 8, *A* and *D*).

Discussion

We have isolated and begun to characterize a gene encoding

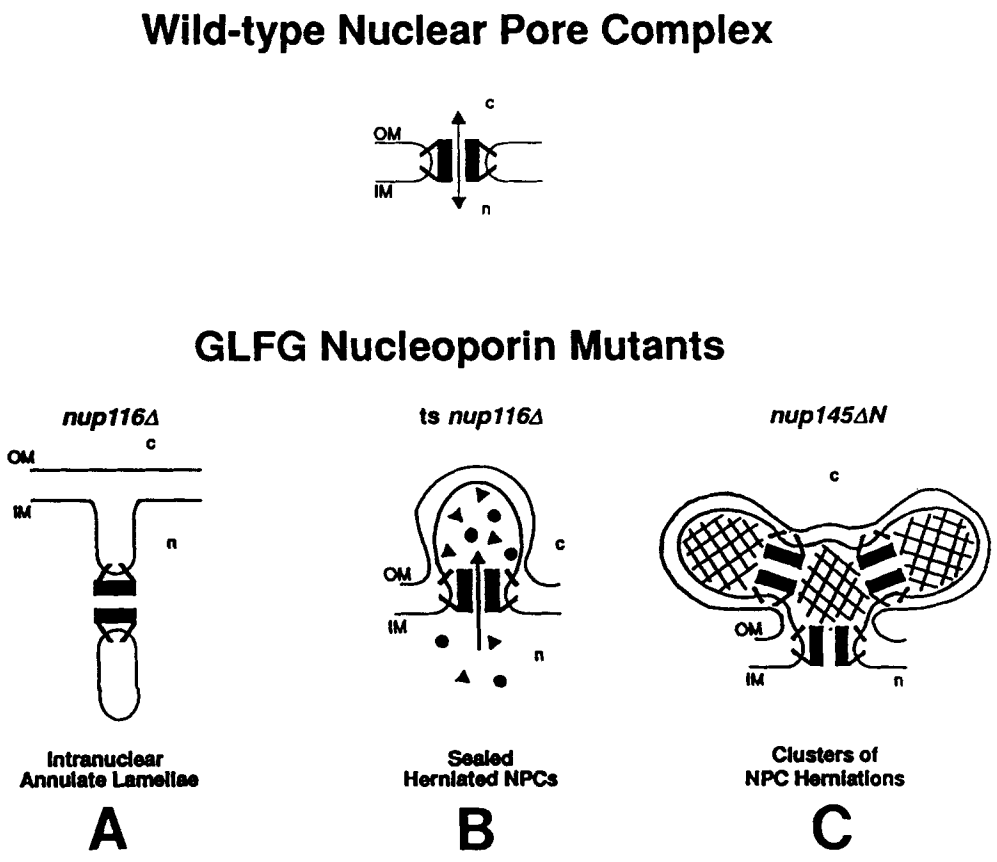

Figure 9. Schematic representation of the NPC/nuclear envelope structures in *nup116Δ* and *nup145ΔN* cells. The invaginations of the inner nuclear membrane that are studded with NPC-like structures are present in *nup116Δ* cells grown at 23 and 37°C (*A*) (Wente and Blobel, 1993). These are remarkably similar in structure to the intranuclear annulate lamellae found in higher eukaryotic cells (Kessel, 1983). At 37°C (*B*), sealed and herniated *nup116Δ* NPCs also appear in the nuclear envelope (Wente and Blobel, 1993). These sealed *nup116Δ* NPCs may continue to transport export substrates that accumulate in the herniation (*closed triangles and circles*). Clusters of NPC-like structures and nuclear envelope extrusions form constitutively in *nup145ΔN* cells at all tested growth temperatures (*C*) (Fig. 6). The filling within the *nup145ΔN* clusters (*hatched*) is indistinguishable from the nucleoplasm, and likely not to represent trapped export substrates as nucleocytoplasmic trafficking is unimpaired in the viable *nup145ΔN* cells. The *nup145ΔN* cluster may originate by a variety of structural perturbations. Shown here is a partial disruption of the interaction of the NPC with the surrounding pore membrane domain. The arrows indicate directionality of nucleocytoplasmic transport. *ts*, temperature sensitive; *IM*, inner nuclear membrane; *OM*, outer nuclear membrane; *n*, nucleus; *c*, cytoplasm.

a fourth member of the yeast GLFG nucleoporin family, *NUP145*. Although at least the amino-terminal half of *NUP145* is not required for cell viability, *nup145ΔN* cells grew slightly slower than their wild-type counterparts and exhibited a striking perturbation of nuclear envelope structure. At light microscopic resolution, *nup145ΔN* cells showed a highly irregular distribution of the NPC immunofluorescence signal, being largely (but not exclusively) located in one or more distinct spots on the nuclear surface (Fig. 5). At electron microscopic resolution these spots correlated with localized clusters of numerous NPC-like structures interconnected by a network of nuclear envelope herniations (Fig. 6, *A–D*).

Such clusters of NPCs have so far not been reported in yeast cells and appear to be distinct from the perturbations we previously reported in *nup116Δ* cells (Wente and Blobel, 1993). Highly schematic versions of the intranuclear annulate lamellae in *nup116Δ* cells (Fig. 9 *A*, present at both 23 and 37°C), the sealed and herniated NPC structures in *nup116Δ* cells grown at 37°C (Fig. 9 *B*), and a small cluster representing the NPC-like structures in *nup145ΔN* cells (Fig. 9 *C*) are shown in Fig. 9. Intranuclear annulate lamellae are not observed in the *nup145ΔN* cells, nor are they structurally similar to the *nup145ΔN* clusters. At first glance, the grape-like NPC clusters in *nup145ΔN* cells appear related to the herniations in temperature-arrested *nup116Δ* cells. However, there are at least two distinguishing characteristics between the *nup145ΔN* and *nup116Δ* phenotypes. First, the individual *nup116Δ* NPCs in the nuclear envelope are apparently sealed by membranous herniations filled with electron-dense material. This sealing blocks nucleocytoplasmic trafficking, although transport of export substrates through the sealed *nup116Δ* NPC and into the herniation may continue. We have suggested that Nup116p is required to anchor the NPC to the pore membrane and thus prevent the inner and outer nuclear membranes from slithering over the pore and fusing. The only slightly diminished growth rate of *nup145ΔN* cells and the lack of electron-dense material accumulating within the *nup145ΔN* clusters suggests that nucleocytoplasmic transport is not significantly impaired in this mutant strain. Therefore, the *nup145ΔN* NPCs are capable of both nuclear import and export and are not sealed like the temperature-arrested *nup116Δ* NPCs.

Secondly, the *nup145ΔN*-herniated NPCs are clustered in an intertangled network whereas the *nup116Δ* herniations are individual. The propensity to form such clusters may be a direct result of at least the absence of the amino-terminal half of Nup145p. Fig. 9 *C* illustrates one of many possibilities, namely that a defect in the attachment of *nup145ΔN* NPCs to the surrounding membrane occurs because this portion of Nup145p interacts with an integral membrane protein of the pore membrane. The weakened structure allows fusion of

the nuclear envelope over the cytoplasmic aspect of an assembling *nup145ΔN* NPC. The clustering would require continued rounds of such defective NPC assembly in the herniated portion of the nuclear envelope. Alternatively, Nup145p may help in anchoring NPCs to a yeast nuclear lamina (Georgatos et al., 1989) or a nuclear envelope lattice (Goldberg and Allen, 1992; Rout and Blobel, 1993). Unanchored, Nup145p-mutant NPCs might then diffuse in the nuclear envelope and aggregate into clusters. The nucleoplasmic basket structures of such unanchored NPCs may also become tangled when opposite sides of the nuclear envelope come together during mitotic extension of the nucleus through the bud neck and into the daughter cell. This could result in clusters of NPCs and nuclear envelope herniations of various sizes (as in Figs. 6 *B*, 8, *A* and *D*), and could account for the limited number of clusters that are randomly positioned with respect to the nucleolus and the spindle pole body. This model assumes that *nup145ΔN* NPCs assemble individually, and then cluster. Still another possibility is that Nup145p provides struts that serve to properly space newly assembled NPCs from one another. In *nup145ΔN* cells the NPCs would assemble too closely together and become aggregated in clusters. Each of these scenarios for *nup145ΔN* cluster formation reflects a unique role for Nup145p in NPC structure and function.

Whereas the *nup116Δ* and *nup145ΔN* mutations resulted in unusual aberrations of nuclear envelope structure, the deletion of *NUP100* had no apparent perturbation on nuclear envelope/NPC ultrastructure in the presence or absence of the *nup145ΔN* mutation (Fig. 8, and Wente et al., 1992). Because of the extensive sequence similarities between these three GLFG nucleoporins (Fig. 1), we genetically tested for possible functional overlaps among Nup145p, Nup100p, and Nup116p. Although cells harboring the *nup100Δ* and *nup145ΔN* mutations are viable, the combination of *nup116Δ* and either *nup100Δ* or *nup145ΔN* resulted in a synthetically lethal strain (Fig. 7). This lethality may reflect a redundancy of Nup116p/Nup100p or Nup116p/Nup145p functions in wild-type yeast cells. However, the strains harboring the *nup116Δ* allele may be so compromised that the addition of any other NPC mutation was lethal. It has also been reported that mutant alleles of *NUP116* are synthetically lethal with a temperature-sensitive allele of *NSP1* (Wimmer et al., 1992). Although the synthetic lethal phenotypes may provide evidence that these nucleoporins are part of the same hetero-oligomeric assembly (the NPC), the precise functional and structural relationships among the individual nucleoporins needs to be further tested by independent means.

We predict that the unique phenotypes of these GLFG nucleoporin mutations reflect overlapping but distinct roles for Nup116p, Nup100p, and Nup145p in NPC structure and function. The herniated NPC-nuclear envelope structures in the *nup116Δ* and *nup145ΔN* cells have pointed to possible roles for Nup116p and Nup145p in maintaining NPC–nuclear envelope interactions and mediating pore complex biogenesis. To precisely delineate their function, our future studies will focus on the substructural localization of GLFG nucleoporins in the NPC, characterization of interactions between GLFG nucleoporins and other proteins in the NPC and pore membrane, and the nature of the interactions between the two distinct p65 and p80 halves of Nup145p.

We would like to thank Eleana Sphicas of the Rockefeller University Electron Microscopy Facility for her expert assistance with the immunoelectron microscopy and EM experiments. The protein sequence data for p65 and p80 was generously provided by Mike Rout and Rick Wozniak (with the assistance of Joseph Fernandez and the Rockefeller University Protein Sequencing Facility). We are grateful to Mike Rout and Susan Smith for their advice and discussions; and to Janis Watkins for assistance with figure preparation. We would also like to thank one of our anonymous reviewers for truly constructive comments and creative interpretations of the *nup145ΔN* ultrastructural phenotype.

S. R. Wente was supported by a National Research Service Award fellowship (1F32GM14268) for part of this work.

Received for publication 3 January 1994 and in revised form 14 February 1994.

References

Altschul, S. F., W. Gish, W. Miller, E. M. Myers, and D. J. Lipman. 1990. Basic local alignment search tool. *J. Mol. Biol.* 215:403–410.

Boeke, J. D., J. Trueheart, G. Natsoulis, and G. R. Fink. 1987. 5-Fluoroorotic acid as a selective agent in yeast molecular genetics. *Methods Enzymol.* 154:164–175.

Byers, B., and L. Goetsch. 1991. Preparation of yeast cells for thin-section electron microscopy. *Methods Enzymol.* 194:602–608.

Davis, L. I., and G. Blobel. 1986. Identification and characterization of a nuclear pore complex protein. *Cell.* 45:699–709.

Davis, L. I., and G. R. Fink. 1990. The *NUP1* gene encodes an essential component of the yeast nuclear pore complex. *Cell.* 61:965–978.

Dayhoff, M. O., W. C. Barker, and L. T. Hunt. 1983. Establishing homologies in protein sequences. *Methods Enzymol.* 91:524–545.

Finlay, D. R., and D. J. Forbes. 1990. Reconstitution of biochemically altered nuclear pores: transport can be eliminated and restored. *Cell.* 60:17–29.

Forbes, D. J. 1992. Structure and function of the nuclear pore complex. *Annu. Rev. Cell Biol.* 8:495–527.

Georgatos, S. D., I. Maroulakou, and G. Blobel. 1989. Lamin A, lamin B, and lamin B receptor analogues in yeast. *J. Cell Biol.* 108:2069–2082.

Goldberg, M. W., and T. D. Allen. 1992. High resolution scanning electron microscopy of the nuclear envelope: demonstration of a new, regular, fibrous lattice attached to the baskets of the nucleoplasmic face of the nuclear pores. *J. Cell Biol.* 119:1429–1440.

Grandi, P., V. Doye, and E. C. Hurt. 1993. Purification of NSP1 reveals complex formation with 'GLFG' nucleoporins and a novel nuclear pore protein NIC96. *EMBO (Eur. Mol. Biol. Organ.) J.* 12:3061–3071.

Greber, U. F., and L. Gerace. 1992. Nuclear protein import is inhibited by an antibody to a lumenal epitope of a nuclear pore complex glycoprotein. *J. Cell Biol.* 116:15–30.

Haltiner, M., T. Kempe, and R. Tjian. 1985. A novel strategy for constructing clustered point mutations. *Nucleic Acids Res.* 13:1015–1025.

Ito, H., Y. Fukuda, K. Murata, and A. Kimura. 1983. Transformation of intact yeast cells treated with alkali cations. *J. Bacteriol.* 153:163–168.

Jones, J. S., and L. Prakash. 1990. Yeast *Saccharomyces cerevisiae* selectable markers in pUC18 polylinkers. *Yeast.* 6:363–366.

Kessel, R. G. 1983. The structure and function of annulate lamellae: porous cytoplasmic and intranuclear membranes. *Int. Rev. Cytol.* 82:181–303.

Kilmartin, J. V., and A. E. M. Adams. 1984. Structural rearrangements of tubulin and actin during the cell cycle of the yeast *Saccharomyces*. *J. Cell Biol.* 98:922–933.

Laemmli, U. K. 1970. Cleavage of structural proteins during the assembly of the head of bacteriophage T4. *Nature (Lond.).* 227:680–685.

Loeb, J. D., L. I. Davis, and G. R. Fink. 1993. NUP2, a novel yeast nucleoporin, has functional overlap with other proteins of the nuclear pore complex. *Mol. Biol. Cell.* 4:209–222.

Miller, M., M. K. Park, and J. A. Hanover. 1991. Nuclear pore complex: structure, function, and regulation. *Physiol. Rev.* 71:909–949.

Mutvei, A., S. Dilmann, W. Herth, and E. C. Hurt. 1992. NSP1 deletion in yeast affects nuclear pore formation and nuclear accumulation. *Eur. J. Cell Biol.* 59:280–295.

Nasymth, K. A., and K. Tatchell. 1980. The structure of transposable yeast mating type loci. *Cell.* 19:753–764.

Nehrbass, U., H. Kern, A. Mutvei, H. Horstmann, B. Marshallsay, and E. C. Hurt. 1990. NSP1: a yeast nuclear envelope protein localized at the nuclear pores exerts its essential function by its carboxy-terminal domain. *Cell.* 61:979–989.

Radu, A., G. Blobel, and R. W. Wozniak. 1993. Nup155 is a novel nuclear pore complex protein that contains neither repetitive sequence motifs nor reacts with WGA. *J. Cell Biol.* 121:1–10.

Reichelt, R., A. Holzenberg, E. L. Buhle, M. Jarnik, A. Engel, and U. Aebi. 1990. Correlation between structure and mass distribution of the nuclear pore complex and of distinct pore complex components. *J. Cell Biol.*

110:883–894.
Rothstein, R. 1991. Targeting, disruption, replacement, and allele rescue: integrative DNA transformation in yeast. *Methods Enzymol.* 194:281–301.
Rout, M. P., and G. Blobel. 1993. Isolation of the yeast nuclear pore complex. *J. Cell Biol.* 123:771–783.
Sambrook, J., E. F. Fritsch, and T. Maniatis. 1989. Molecular Cloning: A Laboratory Manual. Cold Spring Harbor Laboratory, Cold Spring Harbor, New York.
Sanger, F., S. Nicklen, and A. R. Coulson. 1977. DNA sequencing with chain terminating inhibitors. *Proc. Natl. Acad. Sci. USA.* 74:5463–5467.
Schlenstedt, G., E. Hurt, V. Doye, and P. Silver. 1993. Reconstitution of nuclear protein transport with semi-intact yeast cells. *J. Cell Biol.* 123:785–798.
Sherman, F., G. R. Fink, and J. B. Hicks. 1986. Methods in Yeast Genetics. Cold Spring Harbor Laboratory, Cold Spring Harbor, New York.
Sikorski, R. S., and P. Hieter. 1989. A system of shuttle vectors and yeast host strains designed for efficient manipulation of DNA in *S. cerevisiae*. *Genetics.* 122:19–27.
Starr, C. M., M. D'Onofrio, M. K. Part, and J. A. Hanover. 1990. Primary sequence and heterologous expression of nuclear pore glycoprotein p62. *J. Cell Biol.* 110:1861–1871.
Sukegawa, J., and G. Blobel. 1993. A nuclear pore complex protein that contains zinc finger motifs, binds DNA and faces the nucleoplasm. *Cell.* 72:29–38.
Wente, S. R., and G. Blobel. 1993. A temperature-sensitive *NUP116* null mutant forms a nuclear envelope seal over the yeast nuclear pore complex thereby blocking nucleocytoplasmic traffic. *J. Cell Biol.* 123:275–284.
Wente, S. R., M. P. Rout, and G. Blobel. 1992. A new family of yeast nuclear pore complex proteins. *J. Cell Biol.* 119:705–723.
Wilson, I. A., H. L. Niman, R. A. Houghten, A. R. Cherenson, M. L. Connolly, and R. A. Lerner. 1984. The structure of an antigenic determinant in a protein. *Cell.* 37:767–778.
Wimmer, C., V. Doye, P. Grandi, U. Nehrbass, and E. C. Hurt. 1992. A new subclass of nucleoporins that functionally interact with nuclear pore protein NSP1. *EMBO (Eur. Mol. Biol. Organ.) J.* 11:5051–5061.
Wozniak, R., G. Blobel, and M. P. Rout. 1994. POM152 is an integral protein of the pore membrane domain of the yeast nuclear envelope. *J. Cell Biol.* 125:31–42.
Yaffe, M. P., and G. Schatz. 1984. Two nuclear mutations that block mitochondrial protein import. *Proc. Natl. Acad. Sci. USA.* 81:4819–4823.